DOI: 10.1039/c6ra15003a
RSC Advances
Volume 6, Issue 89, 2016, Pages 86269-8627

Supramolecular FRET modulation by pseudorotaxane formation of a ditopic stilbazolium dye and carboxylato-pillar[5]arene

Márton Bojtár,[a] Zoltán Szakács,[b] Dóra Hessz,[c]Fanni L. Bazsó,[d] Mihály Kállay,[e] Miklós Kubinyi[b,c] and István Bitter*[a]

a. Department of Organic Chemistry and Technology, Budapest University of Technology and Economics,1521 Budapest, Hungary

b. Department of Physical Chemistry and Materials Science, Budapest University of Technology and Economics, 1521 Budapest, Hungary

c. Institute of Materials and Environmental Chemistry, Research Center for Natural Sciences, Hungarian Academy of Sciences, 1519 Budapest, P. O. B. 286, Hungary

d. Institute of Organic Chemistry, Research Center for Natural Sciences, Hungarian Academy of Sciences, 1519 Budapest, P. O. B. 286, Hungary

e. MTA-BME Lendület Quantum Chemistry Research Group, Department of Physical Chemistry and Materials Science, Budapest University of Technology and Economics, 1521 Budapest, Hungary

*corresponding author, ibitter@mail.bme.hu

Abstract

In this paper we introduce a new approach towards the modulation of fluorescence resonance energy transfer (FRET). Two stilbazolium dyes (**A**, **D**) exhibiting opposite fluorescence responses

upon complexation with anionic, water soluble carboxylato-pillar[5]arene (**WP5**) were covalently linked via click chemistry, yielding a FRET-capable ditopic indicator (**G**). The pseudorotaxane formation of **G** with **WP5** in pure water induced fluorescence enhancement combined with the modulation of the FRET process due to the interaction of the macrocycle with the two fluorophore units.

Graphical Abstract

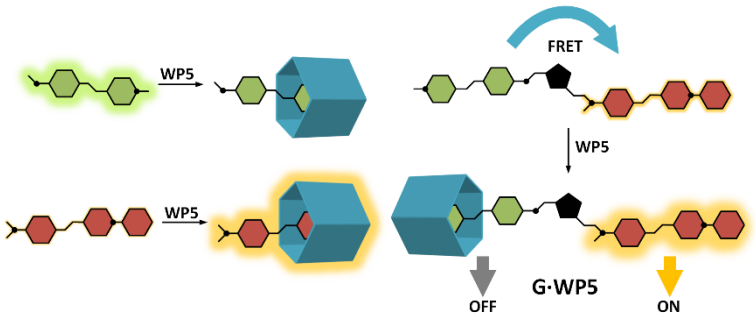

Keywords

FRET, pillararene, stilbazolium dye, pseudorotaxane, macrocycle

1. Introduction

Förster resonance energy transfer (or fluorescence resonance energy transfer, FRET) is an energy transfer mechanism occurring between an excited donor and a ground state acceptor fluorophore through non-radiative dipole-dipole interactions [1, 2]. The efficiency of the FRET process depends on the distance between the donor and acceptor units, on their alignment, on the spectral overlap between the donor emission and the acceptor absorbance and on the fluorescence quantum yield of the donor, thereby providing versatile ways of FRET modulation [3]. FRET is widely used in fluorescence sensing and imaging, utilizing the inherent advantage of ratiometric measurements [4-6]. FRET-related techniques are particularly important in biomedical research, exploiting that FRET is sensitive in the 1-10 nm distance range that matches

the dimensions of proteins, polynucleotides, or the thickness of cell membranes [7-9]. FRET is also popular in the design of chemical sensors, in which the modulation of FRET is achieved by a chemical reaction: the analyte binds covalently or coordinatively to the sensor, induces the splitting of a chemical bond in their donor/acceptor units or induces the cleavage of the donor-acceptor bond [10, 11].

In principle, FRET can also be modulated by supramolecular interactions, in the presence of a macrocyclic host that forms an inclusion complex with the FRET sensor. Stimuli-responsiveness, i. e. photoresponsive supramolecular systems are widely studied [12, 13], especially in the case of interlocked structures [14-16]. A few studies have been published on the effect of cyclodextrins on the fluorescence behavior of FRET dyads in aqueous solutions [17, 18], however the modulation of FRET in covalently linked donor-acceptor pairs by supramolecular interactions is virtually unexplored. In the present work we studied this effect on the example of a complex formed by a stilbazolium dyad (**G**) and a pillararene macrocycle. Since the fluorophore components of **G** are strongly solvatochromic, this could be exploited to modulate the overall FRET process by the changes in optical properties upon interaction with a macrocyclic host. To our knowledge, neither FRET systems containing stilbazolium fluorophores was compiled previously nor the modulation of the intramolecular FRET process was attained by the complexation of a FRET dyad by a pillararene. It was hoped that the results on such a model system can be helpful in the application of solvatochromic FRET-based sensors in complex matrices of biological origin.

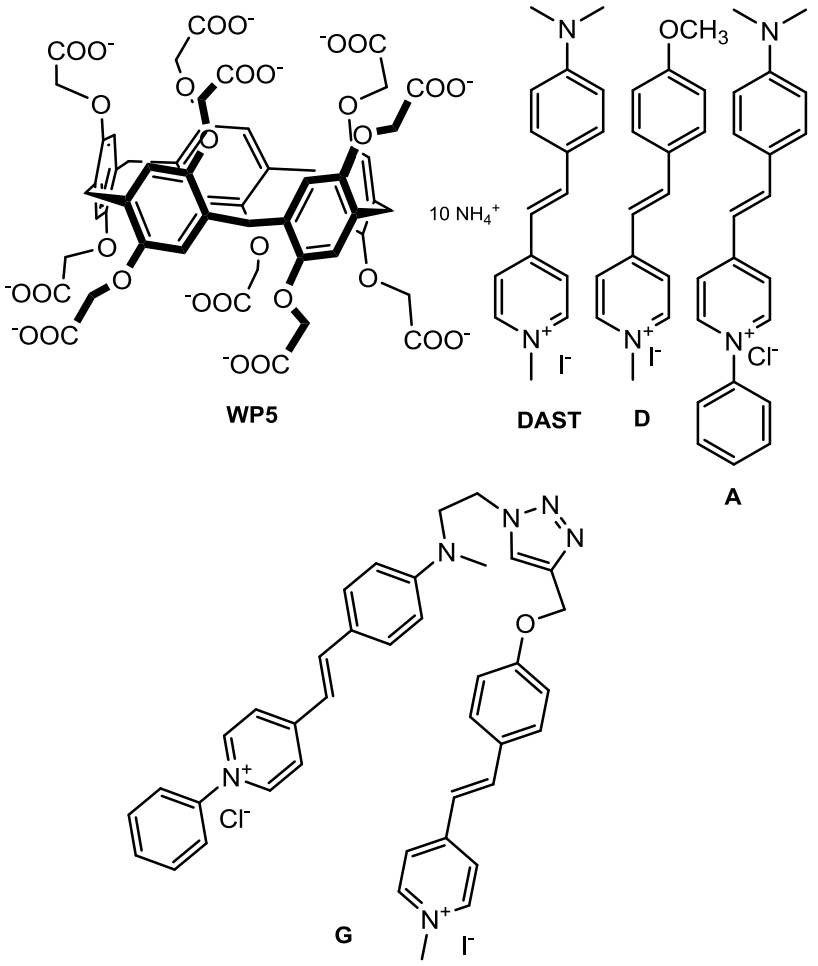

*Fig. 1 Structures of **WP5, DAST, D, A** and **G***

Although pillar[*n*]arenes (**P*n*s**) are a relatively new class of macrocycles [19], they have soon become one of the most popular targets in host-guest chemical studies [20-27]. Especially, the discovery of water soluble derivatives (**WP*n*s**) have further extended their applications in various biological systems. Mostly ionic (carboxylato [28-30], ammonium [31, 32], imidazolium [33]) pillararenes, in particular carboxylato-**P*n*s** have been used in binding studies performed in aqueous medium. Carboxylato-pillar[5]arene (**WP5**), first synthesized by Ogoshi in 2010 [28] is an ideal host for ammonium-containing and electron-deficient guests [34-36]. It is worth mentioning that only a few papers describe the complexation of fluorescent guests by **WP5** [37, 38] and the observation of FRET on sophisticated supramolecular systems containing pillararenes was

reported only in two recent articles [39, 40]. Recently, we described the complexation of **WP5** with three stilbazolium dyes, of which 4-dimethylaminostyryl-*N*-methylpyridinium iodide (**DAST**) produced a colorimetric response and a large fluorescence enhancement upon binding to **WP5** [41]. In the present paper, we report the complexation of two simple pyridinium dyes (**A**, **D**) and their covalently linked, FRET-capable derivative (**G**), with **WP5** (Fig. 1).

2. Results and discussion

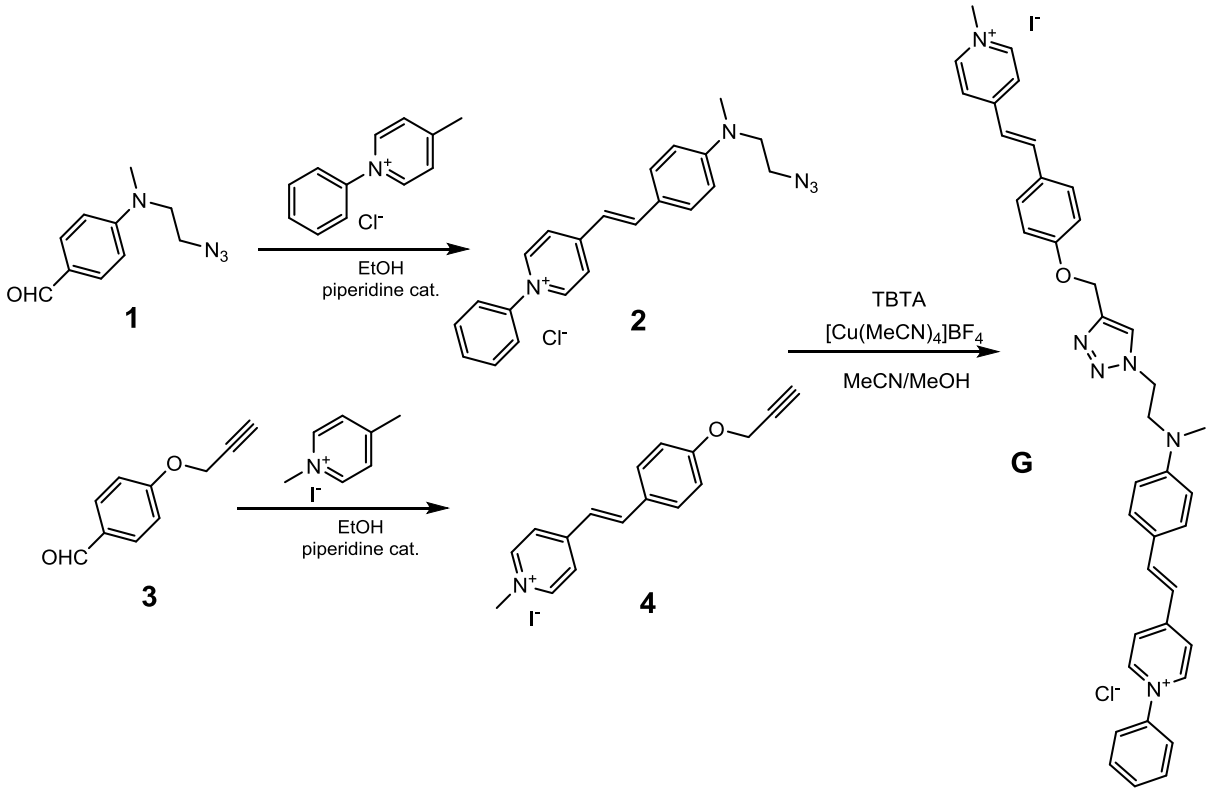

*Fig. 2 Synthetic route towards**G***

2.1 Synthesis

4-Methoxystyryl-*N*-methylpyridinium iodide (**D** as donor), 4-dimethylaminostyryl-*N*-phenylpyridinium chloride (**A** as acceptor) and **WP5** were synthesized using standard literature methods [42-44]. In order to efficiently link these fluorophores, we turned to click chemistry

which is often used to yield FRET-capable dyads [45-48]. The covalently linked ditopic compound was therefore achieved by the click reaction of the *O*-propargyl-analogue of **D** (**4**) and the azide-containing analogue of **A** (**2**) and fully characterized by NMR and HRMS measurements (Fig. 2). The starting materials **2** and **4** were prepared in the same manner as **D** and **A**, namely by the Knoevenagel condensation of the corresponding benzaldehydes **1** and **3**, respectively, in ethanol or methanol using piperidine as catalyst.

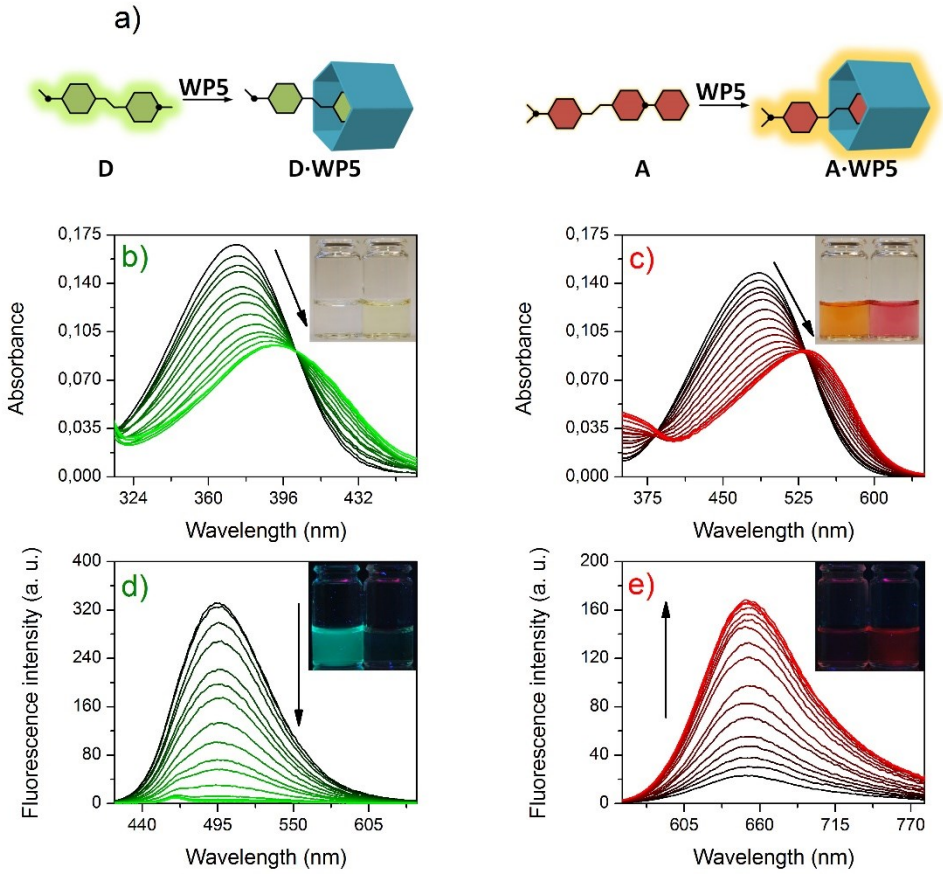

*Fig. 3 (a) Schematic representation of the complexation of **D** and **A** with **WP5**; variation of the (b) absorption and (d) fluorescence (λ_{ex} = 400 nm) spectra of **D** (5.0 μM) in water upon the addition of **WP5** (0 to 2 equivalent); variation of the (e) absorption and (f) fluorescence (λ_{ex} = 530 nm) spectra of **A** (5.0 μM) in water upon the addition of **WP5** (0 to 1.3 equivalent). The insets show*

*the photographs of the corresponding solutions in ambient light and under a UV lamp. The left vials contain only the indicator (20 μM), the right vials the indicator and **WP5** (50 μM)*

2.2 Complexation of D and A with WP5

The effects of the inclusions of **D** and **A** by **WP5** on their fluorescence are illustrated schematically in Fig. 3a. The variations of the absorption and fluorescence spectra of **D** and **A** upon the addition of **WP5** are shown in Figs. 3b-e. They both are negative solvatochromic dyes, accordingly, their absorption bands are shifted to the red when the dyes are included in the pillararene cavity, as an environment of lower polarity (see Figs 3b and 3d). The shifts of the fluorescence bands upon complexation are less pronounced, the intensities, however, show a spectacular change (see Figs. 3c and 3e). Interestingly, despite the virtually small structural differences between **A** and **D**, their fluorescence responses to the complexation are opposite: turn off in case of **D**, turn on in the cases of **DAST** [41] and **A** (see Table 1 for spectroscopic details). The relatively weak fluorescence of uncomplexed **A** can be explained with its deactivation via a low energy twisted intramolecular charge transfer state [49, 50], which is blocked when **A** is confined in the cavity of **WP5**. The fluorescence quenching of **D** upon complexation may berelated with an electron transfer between the pyridinium unit in the excited state of dye and a carboxylate group of the **WP5** host. A photoinduced electron transfer within the contact pair of **DAST** with I^- ion had been described [51]. The theoretically calculated ground state diplole moments for **D** and **A** have close values, but in excited state **D** has a higher dipole moment, which may indicate a higher local positive charge on its pyridinium unit, favoring for electron acception [52].

The expected 1:1 stoichiometries of the **D·WP5** and **A·WP5** complexes were verified by Job's method (see Supporting Information, Figs. S8 and S9). A least-square fitting to the absorption spectra of the dye-pilararene mixtures yielded the values of K_a***(D·WP5)*** = $1.64 \cdot 10^6$ M^{-1} and

K_a(***A·WP5***) = 6.63·10^6 M^{-1} for the association constants. It is clear, that there is no significant difference in the magnitude of the two K_a values.

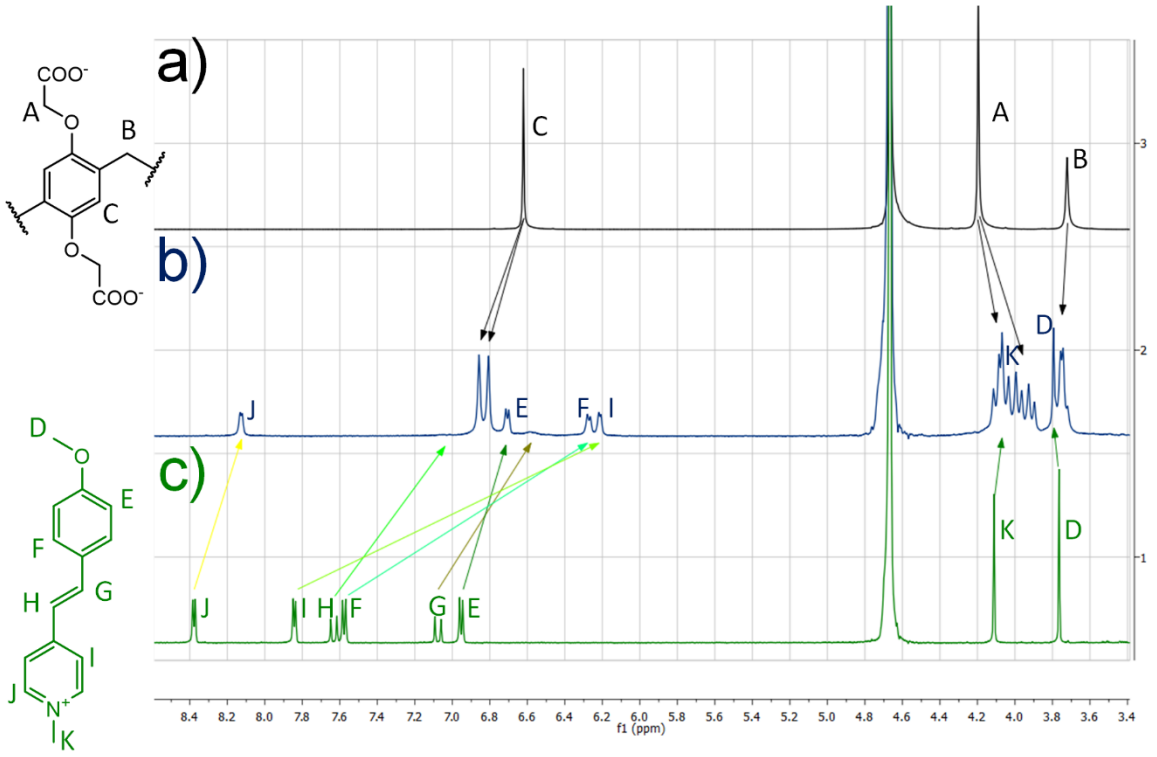

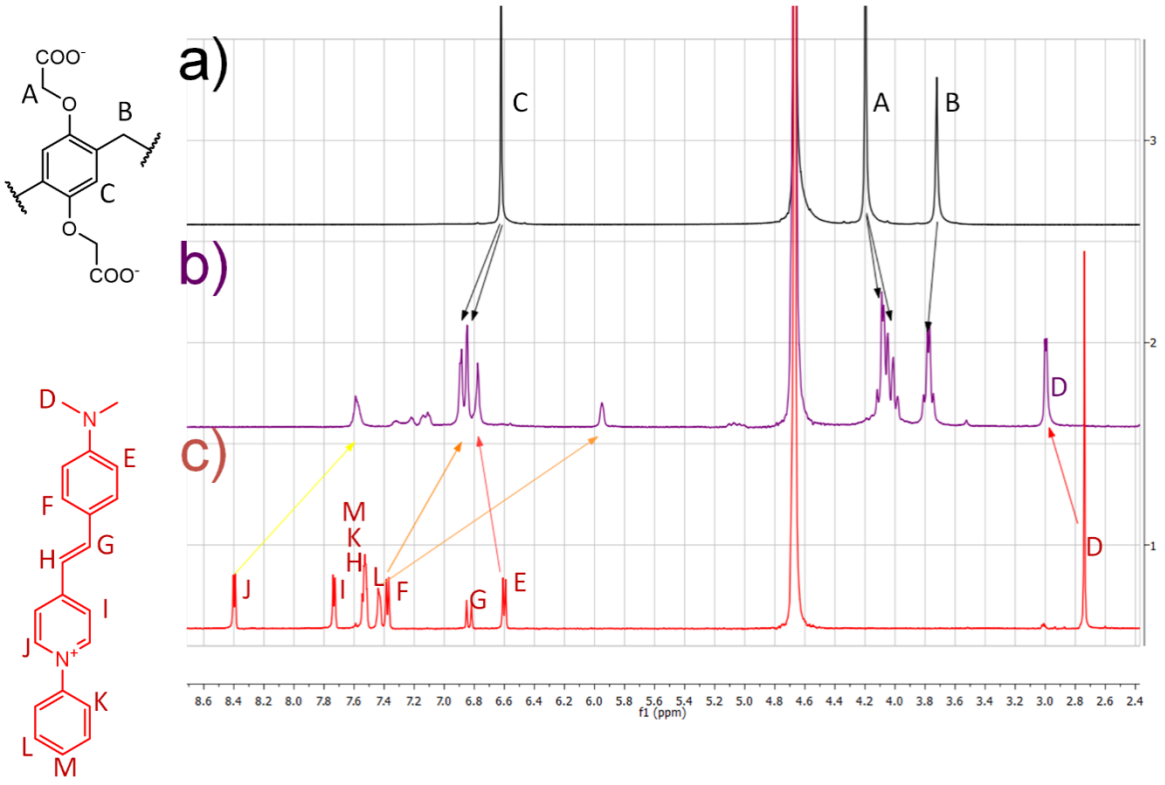

*Fig. 4 ^{1}H-NMR spectra (500 MHz, 25°C) of (top) (**a**) **WP5** (**b**) **D·WP5** (**c**) **D** and of (bottom) (**a**) **WP5** (**b**) **A·WP5** (**c**) **A** (bottom) in D_2O maintaining a constant concentration of 3 mM for all components. Note the splitting of the protons of the host.*

The complexation of **D** and **A** was further examined by ^{1}H NMR spectroscopy in D_2O (Fig. 4). As can be seen on Fig. 4, almost all signals deviate in the spectra of the complexes. The splitting of the proton signals of **WP5** shows the inclusion-induced restriction of rotation (as previously observed with **DAST** and paraquat [21,32]) of the constituent units. Significant upfield shifts and signal broadening can be observed both in the cases of **D** and **A**, that indicate the threading and thereby the shielding effect.

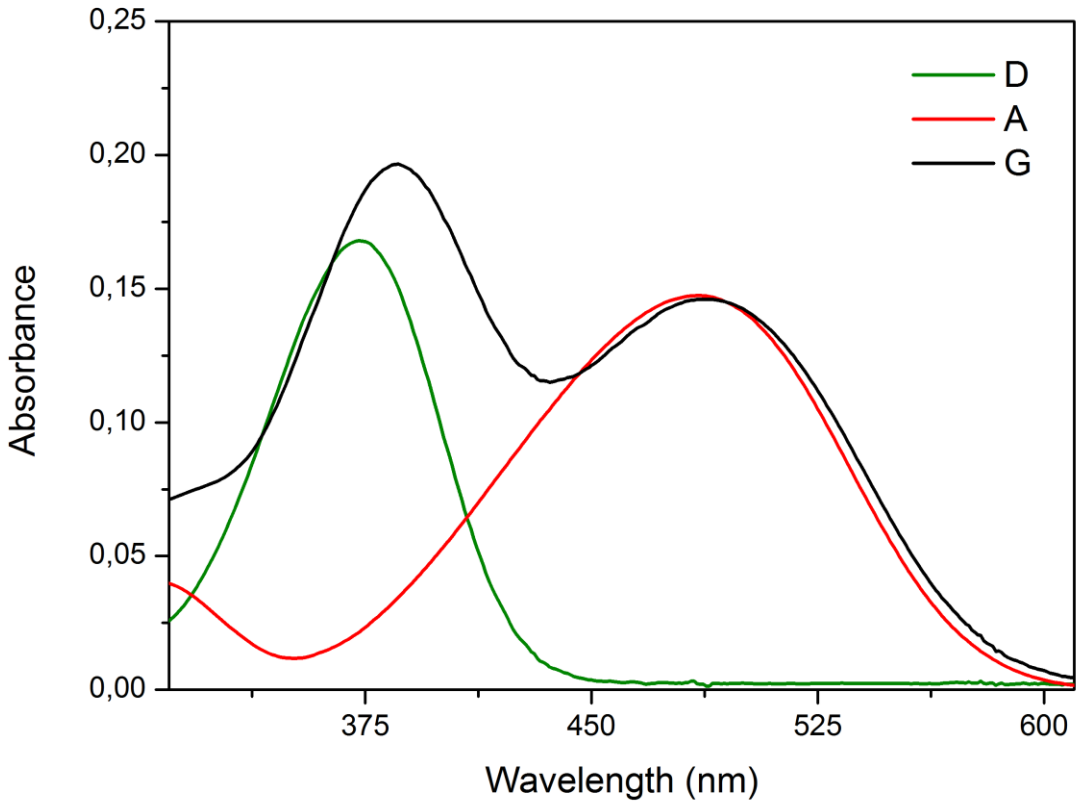

*Fig. 5 Absorption spectra of **D** (green line), **A** (red line) and **G** (black line) in water (5.0 μM)*

2.3 Spectroscopy and complexation of G

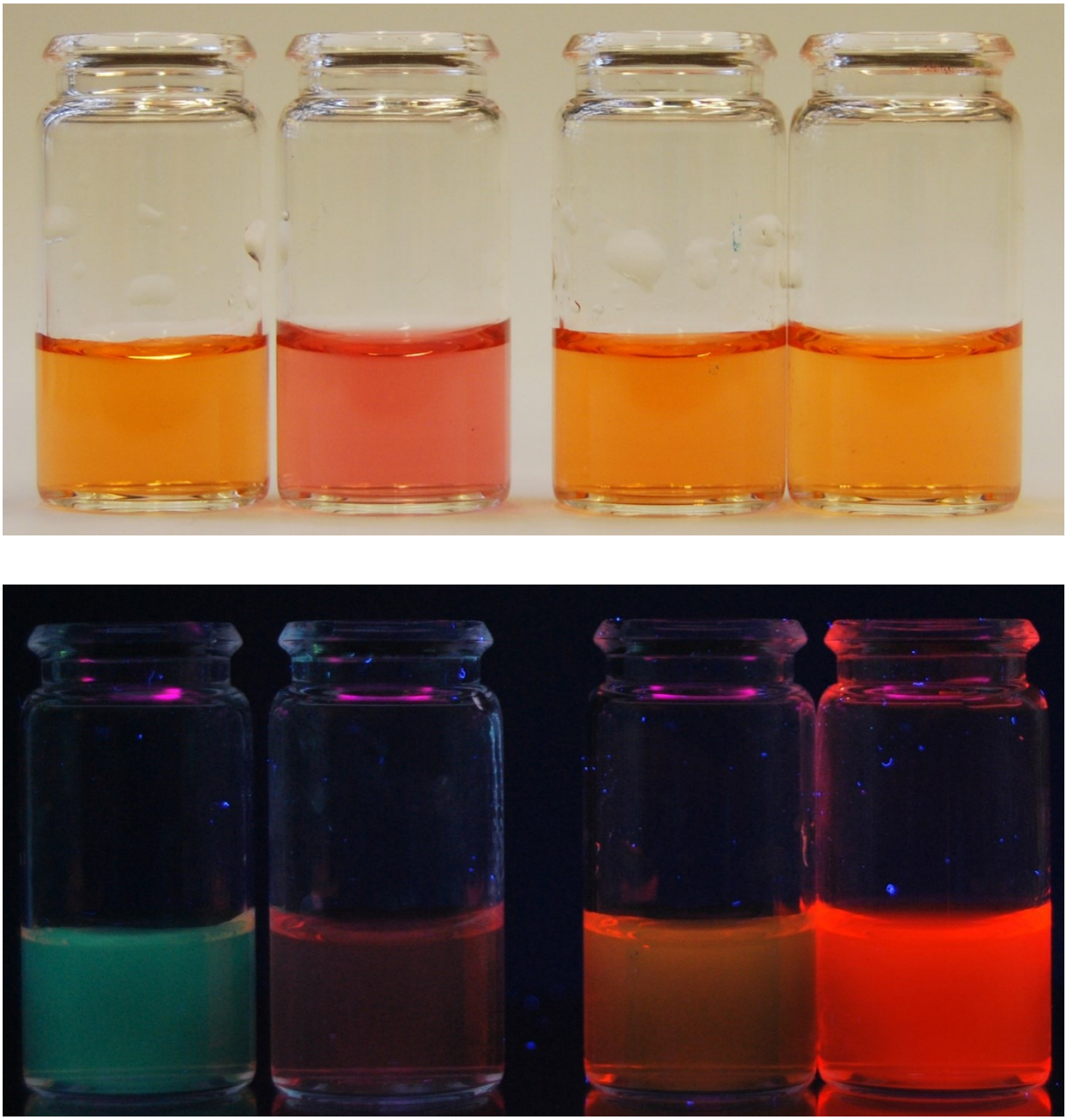

*Fig. 6. The FRET effect of dye **G** and its modulation by **WP5**. The vials contain the aqueous solutions of (from left to right) **D**+**A**; **D**+**A**+**WP5**; **G**; **G**+**WP5**, the upper photographs were taken in ambient light, the lower under UV lamp. The concentrations of **D**, **A** and **G** were 20 μM, the concentration of **WP5** was 50 μM.*

These intriguing results and the ideal overlap of the fluorescence band of **D** and the absorption band of **A** prompted us to synthesize the covalently linked **G**. As expected, **G** shows intense FRET

due to the high level of overlap and the short distance between the fluorophores. The absorption spectrum (Fig. 5) involves two distinct bands, one belonging to the donor, the other to the acceptor part of the molecule. The FRET effect in **G** and the modulation of the FRET via the complexation of **G** by **WP5** are sufficiently strong to be detectable by naked eye, as illustrated in Fig. 6. The FRET process can be clearly seen by comparing the excitation spectra of **G** and **A** (Figs 7a and 7d, black traces): in the spectrum of **G** a new band appears in the absorption range of the donor moiety. As another evidence of FRET, exciting **G** in the absorption range of **D**, the emission of the acceptor componentof the dyad, **G(A)** can be observed beside the emission of its donor moiety, **G(D)** (see Fig. 7b, black trace).

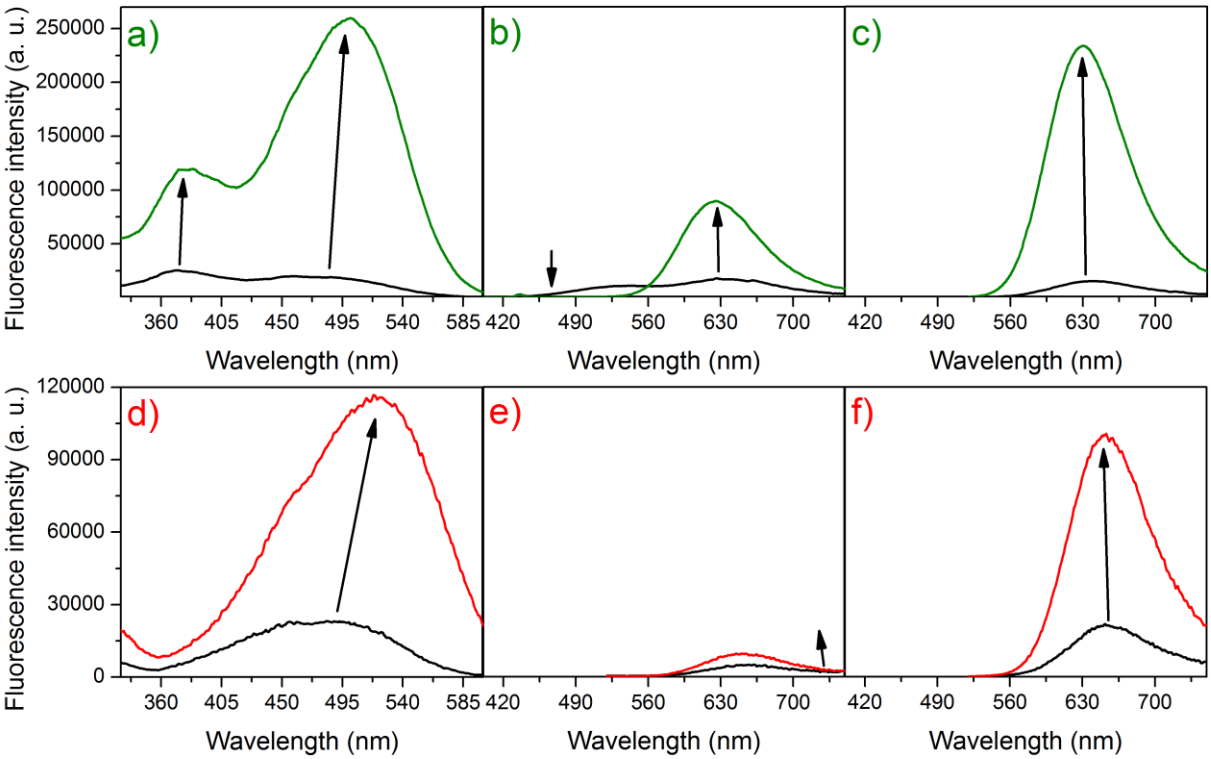

*Fig. 7 (**a-c**) fluorescence spectra of **G** (black) and **G·WP5** (green) compared to (**d-f**) the spectra of **A** (black) and **A·WP5** (red); 5.0 μM dye concentration in water with 2.5 equivalent **WP5** for each. (**a**) and (**d**): excitation spectra λ_{em} = 640 nm; (**b**) and (**e**): emission spectra λ_{ex} = 380 nm; (**c**) and (**f**): emission spectra λ_{ex} = 500 nm*

The addition of **WP5** to the aqueous solution of **G** results in changes in the fluorescence excitation as well as the emission spectrum of **G** (Figs. 7a-c, green traces), which can be considered as the modulation of FRET in the dyad by the supramolecular interactions. The intensity of the fluorescence band belonging to the **G(A)** unit is strongly enhanced, whereas the emission assigned to the **G(D)** moiety is completely quenched – in contrast to the free dyad in which FRET causes only a partial quenching of the **G(D)** emission. In terms of FRET efficiencies,

$$\eta_{FRET} = \frac{\Phi_D - \Phi_{DA}}{\Phi_D}$$

calculated from the fluorescence quantum yields in Table 1, η_{FRET} = 96 % for the free FRET-pair, and increases to 100 % in the complex.

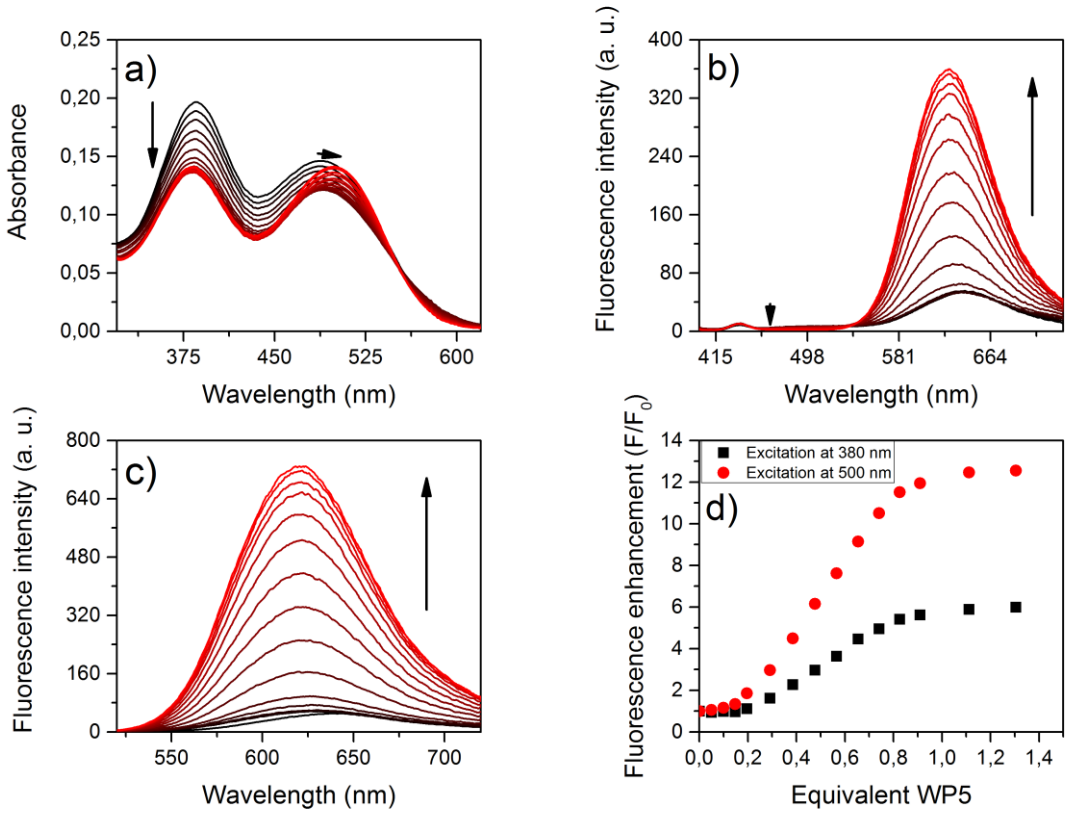

*Fig. 8 Variation of the (**a**) absorption and (**b** and **c**) fluorescence spectra of **G** (5.0 μM) in water upon the addition of **WP5** (0 to 1.3 equivalent),λ_{ex}= (**b**)* 380 nm, (**c**) 500 nm;(**d**) *fluorescence*

*enhancementof **G**, F/F_0, in the presence of **WP5**, measured at λ_{em}= 640 nm, with excitations at λ_{ex}= 380 and 500 nm*

The modulation of FRET arising from the complexation can also be characterized by comparing the fluorescence intensity enhancements of **G** upon the addition of **WP5**, exciting at two wavelengths, one of which (380 nm) falls into the absorption range of the **G(D**) unit, the other (500 nm) in the absorption range of the and **G(A)**moiety (see Fig. 8a). The gradual changes in the fluorescence spectra with the increasing concentration of **WP5** can be followed in Figs. 8b and 8c. As demonstrated in Fig 8d, exciting **G** at the two above wavelengths and measuring the emission at a selected wavelength, the FRET-pair gives a ratiometric response to the addition of **WP5**, with final values of F/F_0(λ_{ex} 380 nm) = 6 for the donor excitation and F/F_0 (λ_{ex}500 nm) = 12.6 for the acceptor excitation.

The variation of the absorption spectrum of **G** (Fig. 8a) with the concentration of added **WP5** (lack of isobestic point, absorbance values show a non-monotonous trend) indicates a multiple product reaction. Assuming the formation of 1:1 and 2:1 complexes, the system can be characterized by the stepwise equilibrium constants K_1 = ***[G·WP5]/[G][WP5]*** and K_2 = ***[G_2·WP5]/[G·WP5][G].*** (As both the donor and the acceptor parts of G may bind to **WP5**, ***[G·WP5]*** and ***[G_2·WP5]*** may be considered as the total concentrations of isomers with the respective compositions.) A least-square fitting to the absorption spectra yielded the values of $K_1 = 4.0\times10^6$ M^{-1} and $K_2 = 4.1\times10^5$ M^{-1}. The sigmoidal shape of the binding isotherm obtained by titrating the solution of **G** with **WP5** (Fig. 8d) is consistent with this reaction scheme (Scheme 1).

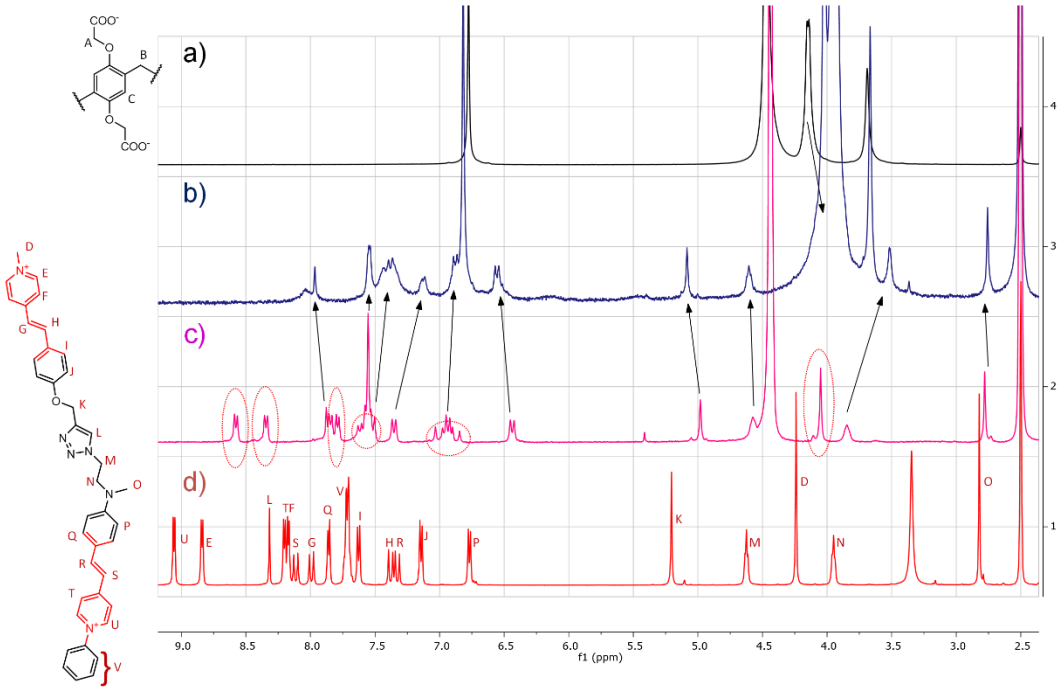

*Fig. 9 ^{1}H-NMR of (a) **WP5** in DMSO-d_6-D_2O 1:1 (3 mM) (b) **G**+**WP5** in DMSO-d_6-D_2O 1:1 (3 mM) at 340 K (c) **G** in DMSO-d_6-D_2O 1:1 (3 mM) (d) **G** in DMSO-d_6 with the assigned protons. The arrows indicate the mainly unchanged proton signals (located at the black parts of the molecule), the red ovals the disappearing proton signals (located at the red part of the molecule)*

The structure of the complex or complexes in the **G·WP5** mixtures was studied with ^{1}H-NMR spectroscopy. Due to the poor solubility of **G** in D_2O, DMSO-d_6-D_2O solvent mixture (1:1 volume ratio) was used at 340 K to avoid the precipitation of **G·WP5**. Thus, an acceptable spectrum was obtained (see Fig. 9) in which some signals of the guest remained more or less unchanged (black arrows, consistent with the black part of the molecule – protons from Kto O and V). However, the pyridinium signals on both ends of the guest disappeared as well as the protons of the double bonds (the dotted red ovals show the disappearing peaks consistent with the red part of the molecule – protons from D to I and from Q to U), while the *N*-phenyl protons seem mostly

unaffected. These qualitative informations allow to assume that the guest can penetrate the macrocycle on both ends followed by threading upon complexation.

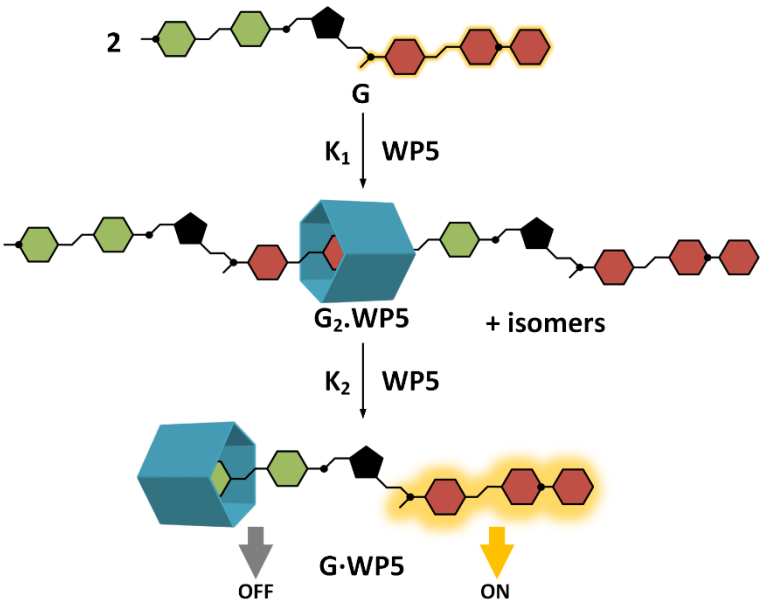

*Scheme 1 Proposed model for complexation of **G** and **WP5***

*Table 1 Optical spectroscopic data of the stilbazolium dyes and their **WP5** complexes*

	λ_{abs} (nm)	ε	λ_{em} (nm)	Φ / Type of excitation
D	373	33602	493	0.0074
D·WP5	392	18967	-	0.00021
A	486	29492	650	0.00018
A·WP5	540	12125	652	0.0017
G	386 490	39336 29206	496 638 638	0.00027 / **D →D** 0.00079 / **D →A** 0.00027 / **A →A**
G·WP5	383 500	28200 28238	- 630	0 / **D →D** 0.0075 / **D →A** 0.0040 / **A →A**

2.4 Computational study on the complexation

To gain a further insight into the structures of **G** and its pseudorotaxane-type complex with **WP5**, theoretical calculations have been carried out (for conformational analyses of rotaxanes see recent articles [53-55]).

The minimal-energy geometries of **G** and **WP5** were searched in two steps. First, we employed a molecular mechanical (MM) conformational analysis using the Merck molecular force field (MMFF94). Thereafter, the conformers with energies up to 8 kJ/mol from the lowest energy conformer were optimized using the PM6-D3H4 (parametrized model 6 with dispersion correction) [56] semi-empirical approach. As could be expected, considering the repulsion of the positive charges on the donor and acceptor parts of **G**, a close-to-linear structure was obtained for the minimum energy conformer (Fig S11a). The minimum of **WP5** was in accordance with its C_5 point group symmetry (Fig. S11b).

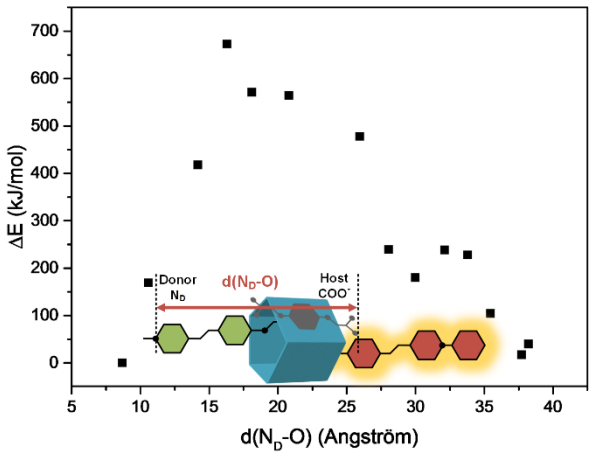

*Fig. 10. The energies of the optimized **G·WP5** complex structures as a function of the averaged $d(N_D\text{-}O)$ distance (distance of the pyridinium N of the donor and the carboxylates on the opposite rim of the macrocycle)*

To analyze the **G·WP5** complex we used the previously optimized geometries of **G** and **WP5** as starting point. We took up 21 initial positions of **G** along the cavity of **WP5**, and optimizing the

geometries with the PM6-D3H4 method 14 different structures were obtained. As shown in Fig. 10 and Table S1 the most favorable structures of the complex were those in which one of the pyridinium terminal groups of **G** protrudes in the cavity of **WP5**, indicating that the complexation is controlled by the Coulomb-interactions. These results are in accord with the NMR measurements. The geometry of the free guest did not change significantly in its **WP5** complex (Fig. S11c-e).

3. Conclusions

In conclusion, we have examined the interaction of stilbazolium dyes **A** and **D** with carboxylato-pillar[5]arene **WP5**. The inclusion complexation resulted in opposite fluorescence responses. The two fluorophores were covalently linked via click chemistry affording a ditopic indicator **G**. To our knowledge, this is the first stilbazolium-based FRET-capable dyad. In water, the pseudorotaxane formation of **G**with**WP5** induced strong fluorescence enhancement which was combined with the modulation of the FRET process, that can be rationalized by the efficient interaction of both fluorophores and the pillararene host. We are currently working on the further understanding of this supramolecular system and the potential application in ratiometric sensing.

4. Materials and methods

4.1 General

Solvents, reagents and starting materials were obtained from commercial supplier and used without further purification. **D** [42], **A** [43], and **WP5** [44]were prepared as described before. All the spectroscopic experiments were carried out at 25°C. The UV−vis absorption spectra were recorded on an Agilent 8453 diode array spectrometer. The fluorescence spectra were measured on an Edinburgh Instruments FLSP 920 fluorescence spectrometer. The ^{1}H NMR spectra were taken on a Bruker Avance DRX-500 spectrometer with chemical shifts reported in ppm (the residual DMSO was used as internal standard). The exact mass measurements were performed

using a Q-TOF Premier massspectrometer (Waters Corporation, 34 Maple St, Milford, MA, USA) using Electrospray ionization in positive mode. The molecular mechanical conformational analysis was carried out using the MarvinBeans program package [57]. The quantum chemical geometry optimizations were performed with the MOPAC 2016 program package [58] .

4.2 Synthetic procedures

4.2.1 Synthesis of 4-(4-((2-(azidoethyl)(methyl)amino)styryl-N-phenylpyridinium chloride (2)

To a mixture of4-((2-azidoethyl)(methyl)amino)benzaldehyde [48] (**1**,330 mg, 1.62 mmol) and *N*-phenyl-4-picolinium chloride [59] (222 mg, 1.08 mmol) in 5 ml refluxing ethanol was added a catalytic amount of piperidine. The reaction mixture was refluxed for 2 hours to reach completion then evaporated. The purple residue was crystallized from acetone and washed with acetone and diethyl ether three times to obtain 280 mg (66%) of **2** as purple crystals. ^{1}H-NMR (500 MHz, DMSO-d_6, 25°C) δ 9.05 (d, *J* = 6.7 Hz, 2H), 8.21 (d, *J* = 6.7 Hz, 2H), 8.13 (d, *J* f= 16.1 Hz, 1H), 7.86 (d, *J* = 7.4 Hz, 2H), 7.76 – 7.64 (m, 5H), 7.35 (d, J = 16.0 Hz, 1H), 6.88 (d, J = 8.6 Hz, 2H), 3.69 (t, J = 5.8 Hz, 2H), 3.55 (t, J = 5.8 Hz, 2H), 3.06 (s, 3H). ^{13}C-NMR (125 MHz, DMSO-d_6, 25°C) δ 154.66, 150.96, 143.52, 143.09, 142.26, 130.69, 130.53, 130.13, 124.17, 122.99, 122.31, 117.24, 112.02, 50.41, 48.36, 38.17. HRMS calculated for $C_{22}H_{22}N_5$ $[M]^+$ *m/z* = 356.1875, found $[M]^+$ 356.1876.

4.2.2 Synthesis of 4-((4-propargyloxy)styryl)-N-phenylpyridinium iodide (4)

To a mixture of 4-propargyloxybenzaldehyde [60] (**3**, 700 mg, 4.37 mmol) and *N*-methyl-4-picolinium iodide (685 mg, 2.91 mmol) in 5 ml refluxing methanol was added a catalytic amount of piperidine. The reaction was refluxed for 2 hours to reach completion then cooled to room temperature and the greenish yellow precipitate was filtered. The crystals were washed with methanol and acetone three times to obtain 881 mg (80%) of **4** as yellow crystals. ^{1}H-NMR (500 MHz, DMSO-d_6, 25°C) δ 8.83 (d, *J* = 6.4 Hz, 2H), 8.19 (d, *J* = 6.4 Hz, 2H), 8.00 (d, *J* = 16.3 Hz, 1H),

7.74 (d, *J* = 8.5 Hz, 2H), 7.40 (d, *J* = 16.3 Hz, 1H), 7.11 (d, *J* = 8.5 Hz, 2H), 4.90 (d, *J* = 2.4 Hz, 2H), 4.25 (s, 3H), 3.64 (t, *J* = 2.4 Hz, 1H). ^{13}C-NMR (125 MHz, DMSO-d_6, 25°C) δ 158.97, 152.72, 144.86, 140.30, 129.81, 128.42, 123.07, 121.11, 115.44, 78.84, 78.56, 55.62, 46.77. HRMS calculated for $C_{17}H_{16}NO$ $[M]^+$ *m/z* = 250.1227, found $[M]^+$ 250.1232.

4.2.3 Synthesis of G

For the click reaction of the azide and alkyne compounds both **2** (81 mg, 0.207 mmol) and **4** (78 mg, 0.207 mmol) were dissolved in 2 ml methanol/4 ml acetonitrile mixture (compound **4** was not completely soluble in methanol). To this solution was added TBTA [61] (11 mg, 10 mol%) and $[Cu(MeCN)_4]BF_4$ (5 mg, 7.5 mol%). This was stirred for 20 hours at room temperature and monitored by TLC (sat. $NH_4Cl_{(aq)}$-MeOH 15:85 on NP-silica). After the completion, the reaction mixture was evaporated and the residue was crystallized from acetone (approx. 15 ml), filtered and washed thoroughly with acetone three times giving 111 mg (70%) deep red crystals. To obtain a high purity product suitable for fluorescence measurements, the product was purified by column chromatography on Al_2O_3 (neutral, Beckmann II) using dichloromethane-methanol 9:1 as eluent. Purifying 64 mg of the product 28 mg of high purity **G** could be obtained (44% yield for the column). ^{1}H-NMR (500 MHz, DMSO-d_6, 25°C) δ 9.03 (d, *J* = 6.5 Hz, 2H), 8.81 (d, *J* = 6.4 Hz, 2H), 8.29 (s, 1H), 8.17 (d, *J* = 6.5 Hz, 2H), 8.14 (d, *J* = 6.4 Hz, 2H), 8.09 (d, *J* = 16.0 Hz, 5H), 7.97 (d, *J* = 16.3 Hz, 1H), 7.83 (d, *J* = 7.1 Hz, 2H), 7.74 – 7.63 (m, 5H), 7.60 (d, *J* = 8.5 Hz, 2H), 7.35 (d, *J* = 16.3 Hz, 1H), 7.30 (d, *J* = 16.0 Hz, 2H), 7.12 (d, *J* = 8.4 Hz, 2H), 6.74 (d, *J* = 8.5 Hz, 2H), 5.18 (s, 2H), 4.60 (t, *J* = 6.1 Hz, 2H), 4.21 (s, 3H), 3.92 (t, *J* = 6.0 Hz, 2H), 2.79 (s, 3H). ^{13}C-NMR (75 MHz, DMSO-d_6, 25°C) δ 160.34, 155.10, 153.27, 151.18, 145.34, 143.95, 143.55, 142.93, 142.72, 140.94, 131.14, 131.00, 130.62, 130.40, 128.56, 125.76, 124.64, 123.52, 122.80, 121.36, 117.76, 115.88, 112.38, 61.74, 51.92, 47.46, 47.21, 38.43. HRMS calculated for $C_{34}H_{36}N_6O$ $[M]^{2+}$ *m/z* = 303.1551, found $[M]^{2+}$ 303.1526

Acknowledgement

We thank the Hungarian Research Foundation for the financial support of this work (Grant No. K108752).

Appendix A supplementary information

Supplementary information (NMR spectra of the compounds, Job's plots, quantum yield determination) is available.

References

[1] Förster T. Zwischenmolekulare Energiewanderung und Fluoreszenz. Ann Phys. 1948;437(1-2):55-75.
[2] Stryer L, Haugland RP. Energy transfer. Spectroscopic ruler. Proc Natl Acad Sci U S A. 1967;58(2):719-26.
[3] J. R. Lakowicz, Principles of Fluorescence Spectroscopy, 3rd Edn., Springer, New York, 2006
[4] Sapsford KE, Berti L, Medintz IL. Materials for fluorescence resonance energy transfer analysis: beyond traditional donor-acceptor combinations. Angew Chem, Int Ed. 2006;45(28):4562-88.
[5] Kobayashi H, Ogawa M, Alford R, Choyke PL, Urano Y. New Strategies for Fluorescent Probe Design in Medical Diagnostic Imaging. Chem Rev. 2010;110(5):2620-40.
[6] Lee MH, Kim JS, Sessler JL. Small molecule-based ratiometric fluorescence probes for cations, anions, and biomolecules. Chem Soc Rev. 2015;44(13):4185-91.
[7] Yin J, Hu Y, Yoon J. Fluorescent probes and bioimaging: alkali metals, alkaline earth metals and pH. Chem Soc Rev. 2015;44(14):4619-44.
[8] Ashton TD, Jolliffe KA, Pfeffer FM. Luminescent probes for the bioimaging of small anionic species in vitro and in vivo. Chem Soc Rev. 2015;44(14):4547-95.
[9] Peng H-Q, Niu L-Y, Chen Y-Z, Wu L-Z, Tung C-H, Yang Q-Z. Biological Applications of Supramolecular Assemblies Designed for Excitation Energy Transfer. Chem Rev. 2015;115(15):7502-42.
[10] Chen X, Pradhan T, Wang F, Kim JS, Yoon J. Fluorescent Chemosensors Based on Spiroring-Opening of Xanthenes and Related Derivatives. Chem Rev (Washington, DC, U S). 2012;112(3):1910-56.
[11] Yuan L, Lin W, Zheng K, Zhu S. FRET-Based Small-Molecule Fluorescent Probes: Rational Design and Bioimaging Applications. Acc Chem Res. 2013;46(7):1462-73.
[12] Li H, Qu D-H. Recent advances in new-type molecular switches. Science China Chemistry. 2015;58(6):916-21.
[13] Qu D-H, Wang Q-C, Zhang Q-W, Ma X, Tian H. Photoresponsive Host–Guest Functional Systems. Chem Rev. 2015;115(15):7543-88.
[14] Yao J, Li H, Xu Y-N, Wang Q-C, Qu D-H. Efficient Intramolecular Energy Transfer between Two Fluorophores in a Bis-Branched [3]Rotaxane. Chemistry – An Asian Journal. 2014;9(12):3482-90.
[15] Cao Z-Q, Miao Q, Zhang Q, Li H, Qu D-H, Tian H. A fluorescent bistable [2]rotaxane molecular switch on SiO2 nanoparticles. Chem Commun. 2015;51(24):4973-6.

[16] Zhang Q, Qu D-H, Wang Q-C, Tian H. Dual-Mode Controlled Self-Assembly of TiO2 Nanoparticles Through a Cucurbit[8]uril-Enhanced Radical Cation Dimerization Interaction. Angew Chem Int Ed. 2015;54(52):15789-93.
[17] Takakusa H, Kikuchi K, Urano Y, Higuchi T, Nagano T. Intramolecular Fluorescence Resonance Energy Transfer System with Coumarin Donor Included in β-Cyclodextrin. Anal Chem. 2001;73(5):939-42.
[18] Alouini M-A, Moustoifa E-F, Rubio-Albenque S, Berthelot T, Fery-Forgues S, Déléris G. Interaction of Fluorescently Labeled Triethyleneglycol and Peptide Derivatives with β-Cyclodextrin. ChemPhysChem. 2014;15(3):444-57.
[19] Ogoshi T, Kanai S, Fujinami S, Yamagishi T-a, Nakamoto Y. para-Bridged Symmetrical Pillar[5]arenes: Their Lewis Acid Catalyzed Synthesis and Host–Guest Property. J Am Chem Soc. 2008;130(15):5022-3.
[20] Cragg PJ, Sharma K. Pillar[5]arenes: fascinating cyclophanes with a bright future. Chem Soc Rev. 2012;41(2):597-607.
[21] Ogoshi T. Synthesis of novel pillar-shaped cavitands "Pillar[5]arenes" and their application for supramolecular materials. J Incl Phenom Macro. 2012;72(3-4):247-62.
[22] Ogoshi T, Yamagishi T-a. Pillararenes: Versatile Synthetic Receptors for Supramolecular Chemistry. Eur J Org Chem. 2013;2013(15):2961-75.
[23] Zhang H, Zhao Y. Pillararene-Based Assemblies: Design Principle, Preparation and Applications. Chem Eur J. 2013;19(50):16862-79.
[24] Strutt NL, Zhang H, Schneebeli ST, Stoddart JF. Functionalizing Pillar[n]arenes. Acc Chem Res. 2014;47(8):2631-42.
[25] Cao D, Meier H. Synthesis of Pillar[6]arenes and Their Host–Guest Complexes. Synthesis. 2015;26(08):1041-56.
[26] Yu G, Wu D, Li Y, Zhang Z, Shao L, Zhou J, et al. A pillar[5]arene-based [2]rotaxane lights up mitochondria. Chem Sci. 2016;7(5):3017-24.
[27] Yu G, Zhou J, Shen J, Tang G, Huang F. Cationic pillar[6]arene/ATP host-guest recognition: selectivity, inhibition of ATP hydrolysis, and application in multidrug resistance treatment. Chem Sci. 2016.
[28] Ogoshi T, Hashizume M, Yamagishi T-a, Nakamoto Y. Synthesis, conformational and host-guest properties of water-soluble pillar[5]arene. Chem Commun. 2010;46(21):3708-10.
[29] Yu G, Xue M, Zhang Z, Li J, Han C, Huang F. A Water-Soluble Pillar[6]arene: Synthesis, Host–Guest Chemistry, and Its Application in Dispersion of Multiwalled Carbon Nanotubes in Water. J Am Chem Soc. 2012;134(32):13248-51.
[30] Shi B, Jie K, Zhou Y, Zhou J, Xia D, Huang F. Nanoparticles with Near-Infrared Emission Enhanced by Pillararene-Based Molecular Recognition in Water. J Am Chem Soc. 2016;138(1):80-3.
[31] Ma Y, Ji X, Xiang F, Chi X, Han C, He J, et al. A cationic water-soluble pillar[5]arene: synthesis and host-guest complexation with sodium 1-octanesulfonate. Chem Commun. 2011;47(45):12340-2.
[32] Jie K, Zhou Y, Yao Y, Shi B, Huang F. CO2-Responsive Pillar[5]arene-Based Molecular Recognition in Water: Establishment and Application in Gas-Controlled Self-Assembly and Release. J Am Chem Soc. 2015;137(33):10472-5.
[33] Yao Y, Li J, Dai J, Chi X, Xue M. A water-soluble pillar[6]arene: synthesis, host-guest chemistry, controllable self-assembly, and application in controlled release. RSC Adv. 2014;4(18):9039-43.
[34] Li C, Shu X, Li J, Chen S, Han K, Xu M, et al. Complexation of 1,4-Bis(pyridinium)butanes by Negatively Charged Carboxylatopillar[5]arene. J Org Chem. 2011;76(20):8458-65.
[35] Li C, Ma J, Zhao L, Zhang Y, Yu Y, Shu X, et al. Molecular selective binding of basic amino acids by a water-soluble pillar[5]arene. Chem Commun. 2013;49(19):1924-6.
[36] Dasgupta S, Chowdhury A, Mukherjee PS. Binding of carboxylatopillar[5]arene with alkyl and aryl ammonium salts in aqueous medium. RSC Adv. 2015;5(104):85791-8.
[37] Wang P, Yan X, Huang F. Host-guest complexation induced emission: a pillar[6]arene-based complex with intense fluorescence in dilute solution. Chem Commun. 2014;50(39):5017-9.

[38] Wang P, Yao Y, Xue M. A novel fluorescent probe for detecting paraquat and cyanide in water based on pillar[5]arene/10-methylacridinium iodide molecular recognition. Chem Commun. 2014;50(39):5064-7.
[39] Ogoshi T, Yamafuji D, Yamagishi T-a, Brouwer AM. Forster resonance energy transfer by formation of a mechanically interlocked [2]rotaxane. Chem Commun. 2013;49(48):5468-70.
[40] Meng L-B, Li D, Xiong S, Hu X-Y, Wang L, Li G. FRET-capable supramolecular polymers based on a BODIPY-bridged pillar[5]arene dimer with BODIPY guests for mimicking the light-harvesting system of natural photosynthesis. Chem Commun. 2015;51(22):4643-6.
[41] Bojtar M, Szakacs Z, Hessz D, Kubinyi M, Bitter I. Optical spectroscopic studies on the complexation of stilbazolium dyes with a water soluble pillar[5]arene. RSC Adv. 2015;5(34):26504-8.
[42] Phillips AP. CONDENSATION OF AROMATIC ALDEHYDES WITH γ-PICOLINE METHIODIDE. J Org Chem. 1949;14(2):302-5.
[43] Coe BJ, Harris JA, Asselberghs I, Clays K, Olbrechts G, Persoons A, et al. Quadratic Nonlinear Optical Properties of N-Aryl Stilbazolium Dyes. Adv Funct Mater. 2002;12(2):110-6.
[44] Kothur RR, Hall J, Patel BA, Leong CL, Boutelle MG, Cragg PJ. A low pH sensor from an esterified pillar[5]arene. Chem Commun. 2014;50(7):852-4.
[45] Fan J, Lin C, Li H, Zhan P, Wang J, Cui S, et al. A ratiometric lysosomal pH chemosensor based on fluorescence resonance energy transfer. Dyes Pigm. 2013;99(3):620-6.
[46] Hu Z, Hu J, Cui Y, Wang G, Zhang X, Uvdal K, et al. A facile "click" reaction to fabricate a FRET-based ratiometric fluorescent Cu2+ probe. Journal of Materials Chemistry B. 2014;2(28):4467-72.
[47] Singh DK, Nath M. meso-Phenyl-triazole bridged porphyrin-coumarin dyads: Synthesis, characterization and photophysical properties. Dyes Pigm. 2015;121:256-64.
[48] Yu Y, Bogliotti N, Maisonneuve S, Tang J, Xie J. Fluorescent dyad for cooperative recognition of copper cation and halogen anion. Tetrahedron Lett. 2013;54(14):1877-83.
[49] Strehmel B, Seifert H, Rettig W. Photophysical Properties of Fluorescence Probes. 2. A Model of Multiple Fluorescence for Stilbazolium Dyes Studied by Global Analysis and Quantum Chemical Calculations. J Phys Chem B. 1997;101(12):2232-43.
[50] Li Z, Sun S, Liu F, Pang Y, Fan J, Song F, et al. Large fluorescence enhancement of a hemicyanine by supramolecular interaction with cucurbit[6]uril and its application as resettable logic gates. Dyes Pigm. 2012;93(1–3):1401-7.
[51] Görner H. Charge transfer fluorescence of trans-stryrylpyridinium iodides. J Photochem Photobiol, A. 2011;218(2–3):199-203.
[52] Han K, Li H, Shen X, Tang G, Chen Y, Zhang Z. Quantum chemistry study on nonlinear optical properties of hemicyanine dye derivatives with different electron donor groups. Comput Theor Chem. 2014;1044:24-8.
[53] Li H, Li X, Ågren H, Qu D-H. Two Switchable Star-Shaped [1](n)Rotaxanes with Different Multibranched Cores. Org Lett. 2014;16(18):4940-3.
[54] Li H, Li X, Cao Z-Q, Qu D-H, Ågren H, Tian H. A Switchable bis-Branched [1]Rotaxane featuring Dual-Mode Molecular Motions and Tunable Molecular Aggregation. ACS Applied Materials & Interfaces. 2014;6(21):18921-9.
[55] Li H, Li X, Wu Y, Ågren H, Qu D-H. A Musclelike [2](2)Rotaxane: Synthesis, Performance, and Molecular Dynamics Simulations. J Org Chem. 2014;79(15):6996-7004.
[56] Řezáč J, Hobza P. Advanced Corrections of Hydrogen Bonding and Dispersion for Semiempirical Quantum Mechanical Methods. J Chem Theor Comput. 2012;8(1):141-51.
[57] MarvinSketch 16.4.25, 2016, ChemAxon (http://www.chemaxon.com)
[58] MOPAC2016, James J. P. Stewart, Stewart Computational Chemistry, Colorado Springs, CO, USA, HTTP://OpenMOPAC.net (2016)
[59] J. Coe B, A. Harris J, Asselberghs I, Persoons A, C. Jeffery J, H. Rees L, et al. Tuning of charge-transfer absorption and molecular quadratic non-linear optical properties in ruthenium(II) ammine complexes [dagger]. J Chem Soc, Dalton Trans. 1999(20):3617-25.
[60] Giguère J-B, Thibeault D, Cronier F, Marois J-S, Auger M, Morin J-F. Synthesis of [2]- and [3]rotaxanes through Sonogashira coupling. Tetrahedron Lett. 2009;50(39):5497-500.

[61] Chan TR, Hilgraf R, Sharpless KB, Fokin VV. Polytriazoles as Copper(I)-Stabilizing Ligands in Catalysis. Org Lett. 2004;6(17):2853-5.